

## Some recent investigations of materials under high pressures

SURINDER M SHARMA

Synchrotron Radiation Section, Bhabha Atomic Research Centre, Mumbai 400 085, India  
E-mail: smsharma@magnum.barc.ernet.in

**Abstract.** By subjecting materials to high pressures one can significantly reduce interatomic and intermolecular distances. This causes drastic changes in the nature of electronic and vibrational states and also in bonding, bringing about several unusual structural, electronic and magnetic phase transitions. In addition, these studies provide a very useful data about the equation of state of the materials of interest. Several examples from our work are presented which elucidate the richness of physics under these conditions.

**Keywords.** High pressure; phase transitions; nanotubes.

**PACS Nos** 62.50.+p; 64.70.Nd

### 1. Introduction

In nature the pressure ranges almost sixty orders of magnitude, lowest being the pressure of hydrogen in the intergalactic space ( $10^{-32}$  bar) and highest in a typical neutron star ( $10^{31}$  bar). In the laboratories the materials can be studied under a pressure higher than at the centre of earth, which is about 3.6 Mbar. Subjecting materials to such high pressures leads to substantial reduction of volume and interatomic distances, which are easily an order of magnitude higher than what is possible with the temperature variation. From the basic physics perspective, this permits studies over a very wide variation of interatomic/intermolecular interactions, providing a more thorough validation of understanding of materials. Understandably, the pressure has a significant effect on the superconductivity – the critical temperature can be tuned [1]. In many materials, magnetically ordered state gets suppressed at high pressures – iron becoming nonmagnetic at  $\sim 12$  GPa [2]. Some intermetallics show coexistence of superconductivity and magnetism under high pressures [3]. High pressure studies are also of geochemical interest, for example, methane production from a mixture of FeO, CaCO<sub>3</sub> and H<sub>2</sub>O has raised hopes of man-made production of natural gas [4]. In addition, such studies provide very useful data on the equation of state of materials. Due to myriad applications of these studies, several laboratories across the world are engaged in the study of materials under high pressures.

Materials under pressures can be studied either by static devices such as diamond anvil cells or other kinds of presses or may be studied under shock loading using a variety of guns or lasers. The main differences between these two techniques are the concomitant temperature increase as well as the higher strain rate increase in the dynamic pressure loading. Due to these reasons, results are sometimes different in shock conditions when compared to static pressure studies. However, methodology exists for inter-comparison of the data obtained from these techniques. In BARC, the studies of materials under high pressures is being carried out for more than three decades employing several experimental and theoretical techniques [5–10]. In this short writeup, a few of the very recent examples of such studies, in which I have been personally involved, are presented.

Most of the experimental studies being presented in this paper have been carried out using diamond anvil cells. This small press comprises of two tiny ( $\sim 0.3$  carat) diamonds forming anvils, on which a metal gasket is mounted and preindented from its initial thickness of  $\sim 250 \mu\text{m}$  to  $\sim 70 \mu\text{m}$ . A hole of  $\sim 100 \mu\text{m}$  is drilled

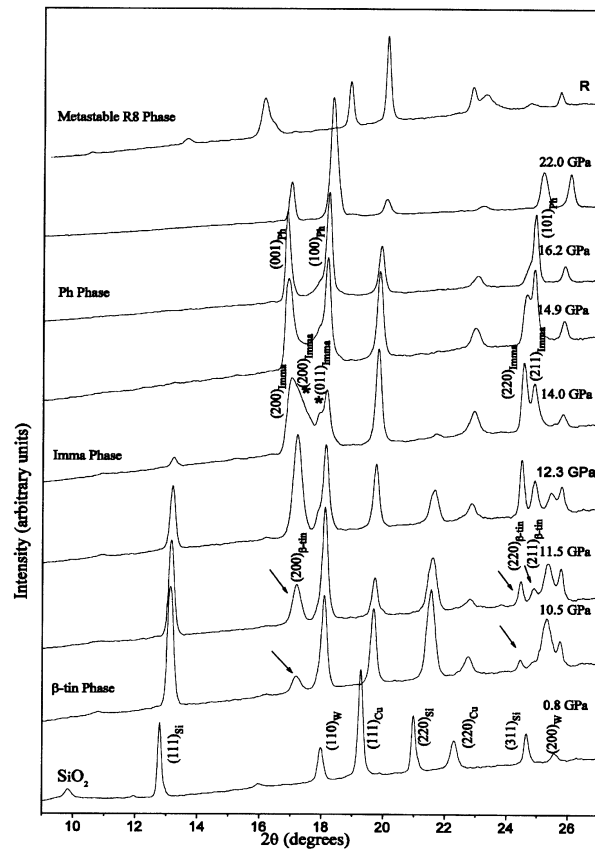


**Figure 1.** X-ray diffraction patterns of Si nanowires under pressure. The diffraction pattern on release of pressure (marked R) can be fitted with R8 structure.

in the centre of this metal sheet which serves as a pressure chamber in which the material for study, a pressure marker (ruby, gold, copper etc.) and pressure transmitting liquid (methanol, ethanol mixture or argon) are loaded. Pressure is raised by pressing the diamonds against each other using an appropriate mechanism. As the typical amount of material of interest is very small ( $\sim$  a few picoliter), these studies require intense sources for measurements. While Raman studies can be carried out using a laser, x-ray diffraction and IR studies require synchrotron sources. Our group has carried out numerous studies using a variety of techniques, a few representative examples of which are given here. All x-ray diffraction studies presented here have been carried out at the synchrotron sources.

## 2. Nanomaterials

### 2.1 *Si nanowires*

Bulk silicon is known to undergo several phase transitions under pressure. For example, cubic diamond phase transforms to tetragonal ( $\beta$ -tin) phase at  $\sim 11$  GPa which sequentially transforms to orthorhombic (Imm) phase at  $\sim 13$  GPa, to primitive hexagonal phase at  $\sim 16$  GPa, to Cmca at  $\sim 38$  GPa, to hcp at 42 GPa and finally to fcc at  $\sim 78$  GPa [11–15]. These transformations are known to be by and large reversible, except that on release of pressure,  $\beta$ -tin phase transforms to BC8 or R8 phase instead of cubic diamond phase [16]. Earlier on we had shown that  $\beta$ -tin – primitive hexagonal phases are related through a soft mode [17], via an intermediate orthorhombic phase, which was discovered later [18].

Our x-ray diffraction (figure 1) and Raman studies on Si nanowires (diameter 70–350 nm) reveal that while cubic phase transforms to the tetragonal phase at lower pressures ( $\sim 7.5$  GPa), other phase transitions, observed up to 22 GPa are more or less in agreement with the results of studies on bulk Si [19]. However, in the cubic phase the shift of Raman modes with pressure, shown in figure 2, have interesting differences from the bulk and porous Si, implying some kind of localization of vibrations.

### 2.2 *Carbon nanotubes*

2.2.1 *Single wall carbon nanotubes.* The behaviour of single wall carbon nanotubes has been investigated under hydrostatic and non-hydrostatic pressures using Raman scattering and x-ray diffraction measurements. Our Raman studies reveal that the pressure transmitter has observable consequences through the interaction of pressure medium with the tubes. Under hydrostatic conditions, x-ray diffraction studies reveal that the tubes continue to retain the two-dimensional translation order up to  $\sim 8$  GPa and lose this order reversibly at  $\sim 9$  GPa [20]. Just before losing the two-dimensional translational order, we observe significant relaxation in the basal plane strain, as shown in figure 3, which is also vindicated by the Raman results [21]. In addition, Raman results show that the radial modes reappear even after release of pressure from  $\sim 26$  GPa. Prior to our studies, a piston cylinder

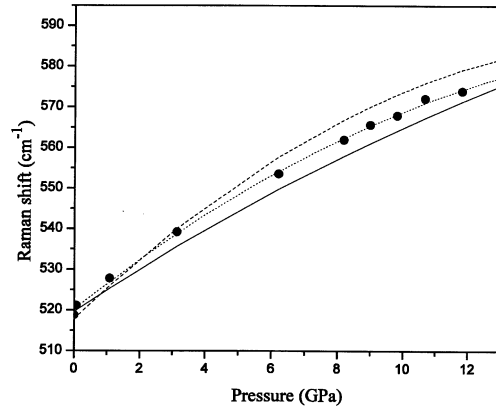


**Figure 2.** Pressure dependence of Raman active mode. Dashed line represents porous Si, dotted line the Si nanowires and solid line the Raman shift in bulk Si.

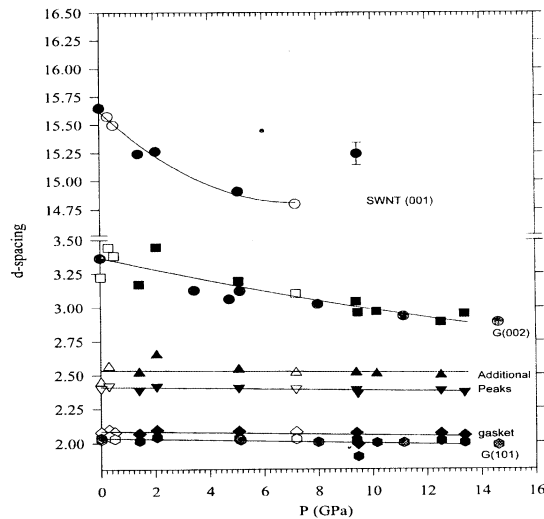


**Figure 3.** Variation of  $d$ -spacings of various diffraction lines with pressure.

study of the compressibility of the tubes had suggested that the tubes are extremely compressible, with a bulk modulus of  $\sim 1$  GPa [22]. Our studies reveal that under hydrostatic pressures, the observed bulk modulus is  $\sim 34$  GPa, i.e. more than an order of magnitude higher than that observed earlier. In addition, the tubes are found to be less compressible compared to even graphite. These results of bulk modulus are in agreement with the model in which tubes act as coupled elastic tubes [23]. Moreover, the compression behaviour observed by us has been found to be compatible with the recent first principles calculations [24]. These studies display the mechanical resilience of these tubes under hydrostatic compression.

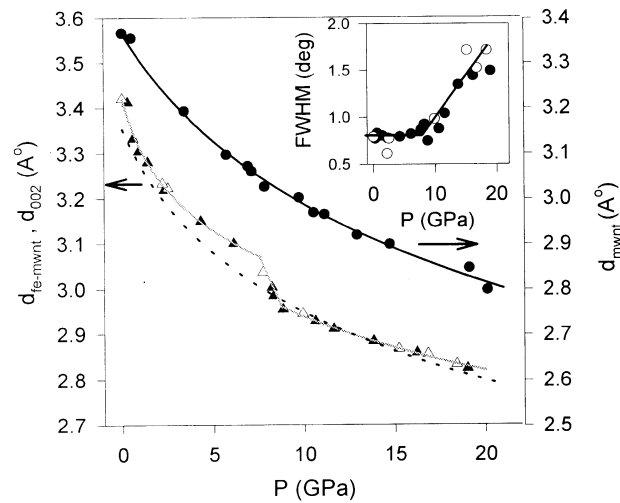


**Figure 4.** Variation of the average intershell distance  $d_0$  of Fe-filled MWNTs with pressure. Solid triangles indicate increasing pressure and open triangles indicate decreasing pressure, and pristine MWNT is indicated by solid circles. Variation of  $d_{002}$  line of graphite (dash line) is also plotted for comparison. For the sake of clarity, the left side of  $y$ -axis is for the filled tubes and graphite, whereas the right side is for pristine tubes. The inset shows variation of the linewidth of the MWNT diffraction line for iron-filled MWNT.

Under non-hydrostatic pressures (no pressure transmitting fluid) the compressibility of these nanotubes is found to be almost twice when compared to the results of hydrostatic compression [25]. Under these conditions, x-ray diffraction results show that the tubes lose the translation order at  $\sim 2$  GPa and this change is reversible up to  $\sim 6$  GPa and becomes irreversible beyond that pressure. The pressure-induced Raman shifts confirm these results and also show that the tubular nature re-emerges on release of pressure from even 30 GPa while x-ray diffraction results imply that the translational periodicity, characteristic of a bundle does not re-emerge from the release of pressure from such high terminal pressures. Moreover, comparison of these results with other measurements [26,27], claimed to have been carried out at hydrostatic compressions, indicate that the phase transition observed at  $\sim 1.75$  GPa as well as reversibility from the compression under 4 GPa may be due to the non-hydrostatic pressures.

**2.2.2 Fe-filled carbon multi-wall tubes.** The recorded x-ray diffraction of the Fe-filled multi-wall nanotubes show that the diffraction pattern has three components, viz., due to multi-wall tubes, bcc iron and interfacial  $\text{Fe}_3\text{C}$  with the relative abundances of 54:36:9 [28]. High pressure behaviour of pristine multi-wall tubes is also investigated and these studies show that these multi-wall carbon nanotubes (MWNTs) do not undergo any phase transition up to 20 GPa, though these gradually become amorphous beyond 10 GPa. Figure 4 summarizes the results of our observations.

Bcc iron in the tubes also shows no phase transition up to 20 GPa, in contrast with the bulk iron which undergoes a bcc to hcp phase change at  $\sim 12$  GPa [28].

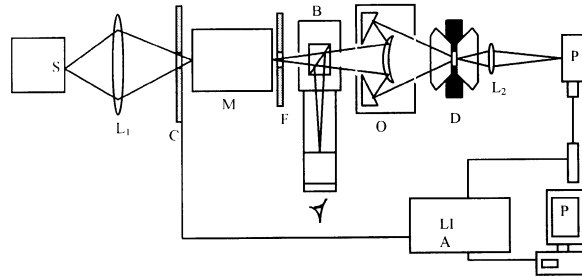


**Figure 5.** Schematic representation of high pressure optical absorption set-up.

However, Fe-filled tubes and  $\text{Fe}_3\text{C}$  undergo a simultaneous phase change at  $\sim 9$  GPa. Iso-structural phase transformation observed in  $\text{Fe}_3\text{C}$  at 9 GPa is in contrast with the behaviour of bulk  $\text{Fe}_3\text{C}$  which shows no structural change up to  $\sim 70$  GPa [29]. In addition, bcc iron as well as  $\text{Fe}_3\text{C}$  are far more compressible than their bulk counterparts as reflected in their bulk moduli which are 90 GPa (170 GPa) and 135 GPa (175 GPa), where the numbers in the parenthesis indicate the values for the bulk.

### 3. Scheelite compounds

There are several alkaline earth molybdates and tungstates which crystallize at ambient conditions in the tetragonal layered structure with space group  $I4_1/a$ . These compounds are known to have several applications such as scintillators, laser host materials, cryogenic detectors for dark matter etc. Earlier high pressure studies, based on packing considerations, suggested that these materials would transform to a monoclinic wolframite structure [30]. Several recent investigations suggest that under high pressures these could transform to wolframite [31], fergusonite [32] or  $\text{HgMoO}_4$  [33] structure. We have investigated the high pressure behaviour of two of these compounds, namely  $\text{BaWO}_4$  [34] and  $\text{BaMoO}_4$  [35]. Raman and x-ray diffraction measurements show that both these compounds transform at  $\sim 6$ – $8$  GPa, to a denser phase, the structure of which is unambiguously fergusonite. At still higher pressures these undergo another phase change to a structure which has a monoclinic cell but the structure of which is inconsistent with recent first principles calculations [36].

### 4. Light absorption experiments under pressure

To study the variation in the band gap of the materials under pressure, we have set up light absorption experiments [37], the schematic of which is given in figure 5. This instrument is able to focus monochomatized light onto a single crystal in a diamond anvil cell to  $\sim 10 \mu\text{m}$ , as shown in figure 6.

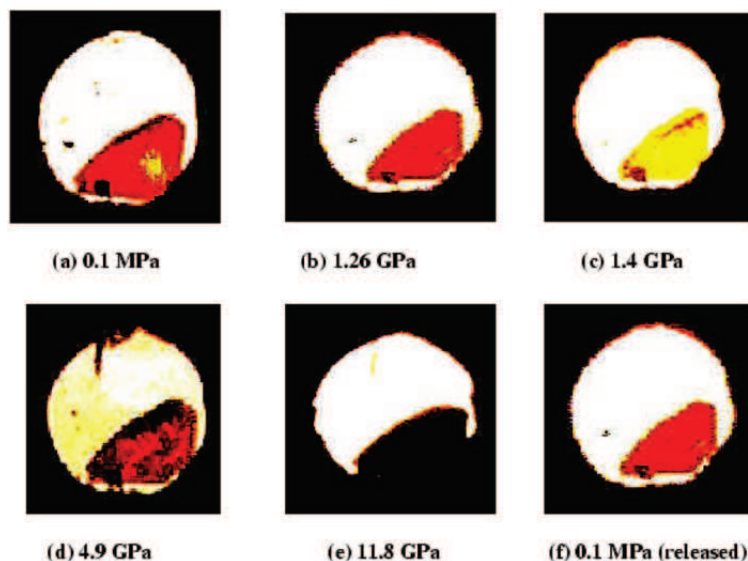


**Figure 6.** Microphotographs of HgI<sub>2</sub> single crystal in the gasketed diamond anvil cell taken at different pressures (a–f). The circular spot in (a) indicates the typical size of the monochromatic beam focused onto the sample. At 1.3 GPa initially red crystal turns yellow.

Our study on HgI<sub>2</sub>, a layered compound, shows that it undergoes two phase transformations [37]. The tetragonal to orthorhombic phase transformation, observed at 1.4 GPa, is accompanied by an abrupt increase in the band gap while the nature of the gap does not change. However, across the orthorhombic to hexagonal phase transformation, observed at 7.2 GPa, the gap decreases discontinuously and changes from direct to indirect type. These studies suggest that HgI<sub>2</sub> may metallize at 40 GPa, if not prevented by any other structural change. The observed changes in the band gaps are shown in figure 7.

## 5. Germania

GeO<sub>2</sub> is an important geophysical material, partly due to several similarities of its behaviour to SiO<sub>2</sub> [38]. Recent studies show that  $\alpha$ -GeO<sub>2</sub>, having quartz structure transform to a monoclinic phase at high pressures [39]. Vitreous form of GeO<sub>2</sub> has been claimed to transform to the denser phase through a state in which Ge is coordinated with five oxygen atoms [40]. In addition, another investigation claimed that melt GeO<sub>2</sub> transforms to a denser liquid phase under pressure [41]. So as to gain insight into the mechanism of these changes, molecular dynamics simulations were carried out on various phases of GeO<sub>2</sub> [42].

Our results show that  $\alpha$ -GeO<sub>2</sub> transforms to the  $\beta$ -quartz form at  $\sim 1050$  K and it melts at 1500 K. Agreements of these results indicate that the pair potentials [38] being used in these simulations are reasonable for studying the structural variations.

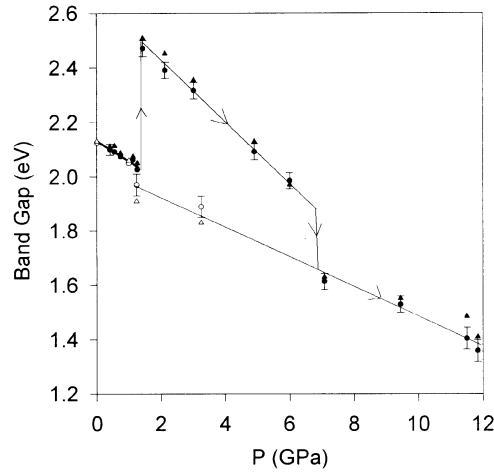


**Figure 7.** Pressure dependence of the band gap in HgI<sub>2</sub>. Band gap increases abruptly at 1.4 GPa (direct–direct transition) followed by another (direct–indirect transition) at ~7.0 GPa. Upon release of pressure, the observed changes in the gap do not retrace the changes observed on pressure increase.

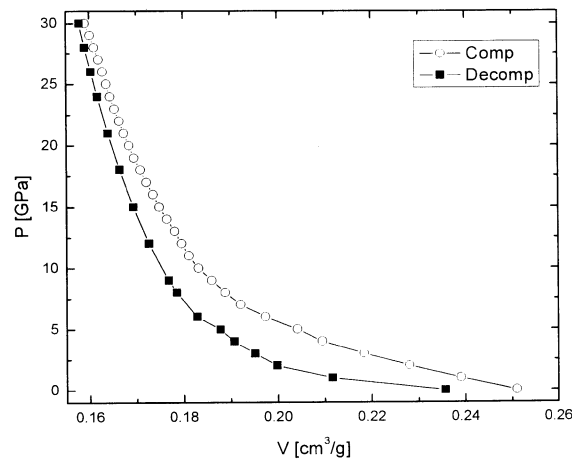


**Figure 8.** Variation of volume with pressure for vitreous GeO<sub>2</sub> at 300 K.

Our simulations under high pressures show that at ~9 GPa,  $\alpha$ -GeO<sub>2</sub> transforms to a partially disordered structure, the diffraction pattern of which is in reasonable agreement with the experimentally observed monoclinic structure. The Ge–O coordination number increases smoothly but Ge is not fully six-coordinated even at 20 GPa.

Vitreous GeO<sub>2</sub> was generated by rapid cooling of the liquid phase from 3500 K, and its computed partial structure factors agree well with the experimental results. Subjecting this phase to high pressures lead to systematic (and almost reversible) densification (figure 8) and in the denser phase Ge–O coordination increases as

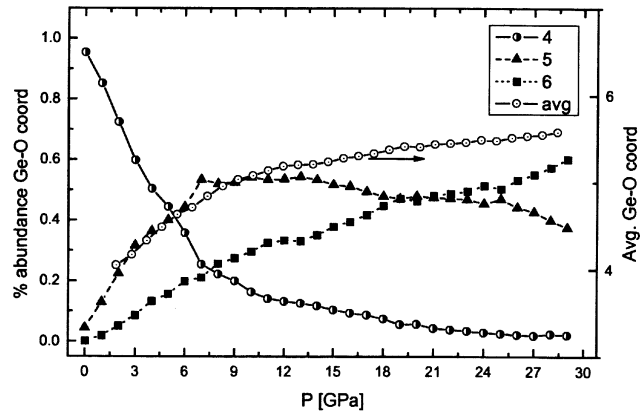


**Figure 9.** Variation of fractional abundance Ge–O coordination with pressure for vitreous GeO<sub>2</sub> at 300 K.

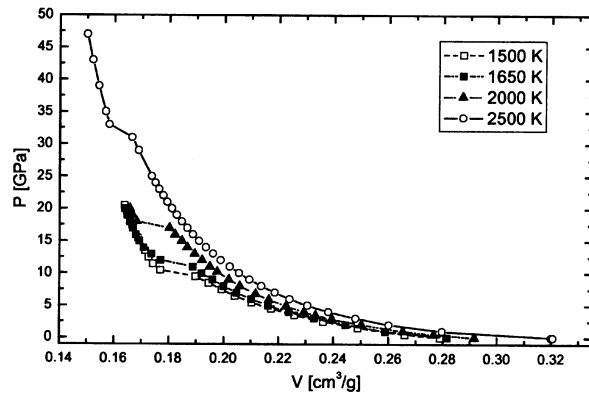


**Figure 10.** Variation of the volume of molten GeO<sub>2</sub> on increase of pressure at 1500, 1650, 2000 and 2500 K.

shown in figure 9. Our simulations show that although almost 50% Ge are coordinated to five oxygen atoms, the average coordination shows no plateau at five coordination (figure 9), raising a doubt on the claims of observance of five coordinated stable state at high pressures. Coordination number increases smoothly up to ~30 GPa to a value of 5.6. On release of pressure, the densified phase smoothly transforms back to almost octahedrally coordinated phase.

Liquid phase transforms to a denser phase when subjected to pressures which increase with the temperature of the initial liquid phase. This first-order phase transition is also accompanied by an abrupt increase in Ge–O coordination and hence increase in Ge–O bond length, as observed in the experiments [41]. The computed variations are shown in figures 10–12.

We characterize the nature of higher pressure phase by evaluating the shear rigidity of the new phase. While the starting liquid phase has no shear rigidity, the denser high pressure phase is found to have the shear rigidity indicating that it

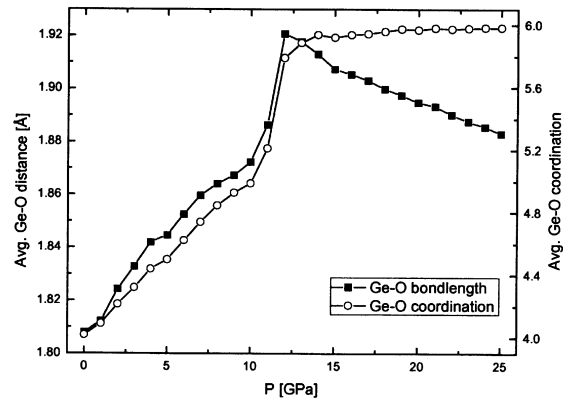


**Figure 11.** Variation of Ge–O distance and coordination for the initial liquid phase with pressure.

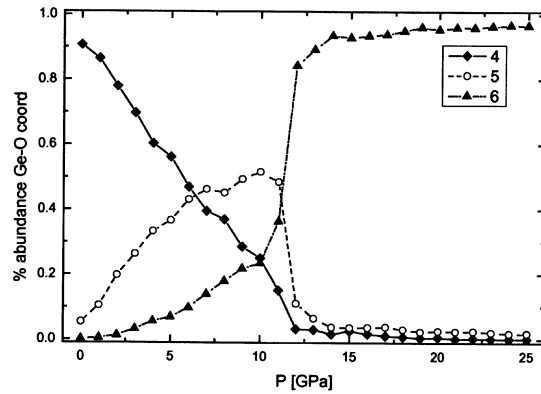


**Figure 12.** Variation of fractional abundance of Ge–O coordination with pressure for the phase which was liquid at 1650 K.

may be a solid glassy phase rather than a denser liquid phase. These results should encourage more careful experiments on the liquid phase.

### Acknowledgements

It is a pleasure to acknowledge my collaborators Himanshu Poswal, S Karmakar, Nandini Garg, Vinod Panchal, K Shanavas, Dr Pallavi V Teredesai, Prof. Ajay Sood, Prof. C N R Rao and Dr S K Sikka. Constant encouragement from Dr R Chidamabaram and Dr V C Sahni is also thankfully acknowledged.

### References

- [1] L Gao *et al*, *Phys. Rev.* **B50**, 4260 (1994)
- [2] G S Eumann, L Sixtrude and R E Cohen, *Proc. Natl Acad. Sci. (USA)* **101**, 33 (2004)

- [3] D Jaccard *et al*, *Physica* **B230–232**, 297 (1997)
- [4] H P Scott, Russell J Hemley, H K Mao, D R Herschbach, L E Fried, W M Howard and Sorin Bastea, *PNAS* **101**, 14023 (2004)
- [5] R Chidambaram and Surinder M Sharma, *Curr. Sci.* **60**, 397 (1991)
- [6] R Chidambaram and Surinder M Sharma, *Bull. Mater. Sci.* **22**, 153 (1999)
- [7] S K Sikka and Surinder M Sharma, *Proc. Ind. Natl Sci. Acad.* **A68**, 293 (2002)
- [8] Surinder M Sharma and S K Sikka, *Prog. Mater. Sci.* **40**, 1 (1996)
- [9] Surinder M Sharma, in *Disordered materials* edited by S Prakash, N Goyal and S K Tripathi (Norosa Publishing House, New Delhi, 2003) pp. 81–90
- [10] S K Sikka, B K Godwal and R Chidambaram, in *High pressure shock compression of solids III* edited by Lee Davison and Mohsen Shahinpoor (Springer-Verlag, New York, 1998) pp. 1–30.
- [11] J C Jamieson, *Science* **139**, 762 (1963)
- [12] H Olijnyk, S K Sikka and W B Holzapfel, *Phys. Lett.* **A103**, 137 (1984)
- [13] M I McMahan and R J Nelmes, *Phys. Rev.* **B47**, 8337 (1993)  
M I McMahan, R J Nelmes, N G Write and D R Allan, *Phys. Rev.* **B50**, 739 (1994)
- [14] M Hanfland, U Swarz, K Syassen and K Takemura, *Phys. Rev. Lett.* **82**, 1197 (1999)
- [15] J Duclos, Y K Vohra and A L Ruoff, *Phys. Rev. Lett.* **58**, 8 (1987)
- [16] R H Wentorf and J S Kasper, *Science* **139**, 338 (1963)  
F P Bundy, *J. Chem. Phys.* **41**, 3809 (1964)
- [17] S M Sharma and S K Sikka, *J. Phys. Chem. Solids* **46**, 477 (1985)
- [18] J Crain, G J Ackland, J R Maclean, R O Piltz, P D Hatton and G S Pawley, *Phys. Rev.* **B50**, 13043 (1994)
- [19] H K Poswal, Nandini Garg, Surinder M Sharma, E Busetto, S K Sikka, Gautam Gundiah, F L Deepak and C N R Rao, *J. Nanosci. Nanotech.* **5**, 729 (2005)
- [20] Surinder M Sharma, S Karmakar, S K Sikka, P V Teredesai, A K Sood, A Govindarajan and C N R Rao, *Phys. Rev.* **B63**, 205417 (2001)
- [21] P V Teredesai, A K Sood, D V S Muthu, R Sen, A Govindaraj, C N R Rao, *Chem. Phys. Lett.* **319**, 296 (2000)
- [22] S A Chesnokov, V A Nalimova, A G Rinzler, R E Smalley and J E Fischer, *Phys. Rev. Lett.* **82**, 343 (1999)
- [23] V N Popov *et al*, *Solid State Commun.* **114**, 395 (2000)
- [24] S Riech, C Thomson and P Ordejon, *Phys. Rev.* **B65**, 153407 (2002)
- [25] S Karmakar, S M Sharma, P V Teredesai, D V S Muthu, A Govindaraj, S K Sikka and A K Sood, *New J. Phys.* **5**, 143 (2003)
- [26] J Tang, L C Qin, T Sasaki, M Yudasaka, A Matsushita and S Iijima, *Phys. Rev. Lett.* **85**, 1887 (2000)
- [27] S Rols, I N Gontcharenko, R Almirac, J L Sauvajol and I Mirebeau, *Phys. Rev.* **B64**, 153401 (2001)
- [28] S Karmakar, S M Sharma, P V Teredesai and A K Sood, *Phys. Rev.* **B69**, 165414 (2004)
- [29] J Li, H K Mao, Y Fei, E Gregoryanz, M Eremets and C S Zha, *Phys. Chem. Minerals* **29**, 166 (2002)
- [30] A W Sleight, *Acta Crystallogr.* **B28**, 2899 (1972)
- [31] A Jayaraman, S Y Wang and S K Sharma, *Phys. Rev.* **B52**, 9886 (1995)
- [32] A Grzechnik, K Syassen, I Loa, M Hanfland and J Y Gesland, *Phys. Rev.* **B65**, 104102 (2002)
- [33] A Jayaraman, B Batlogg and L G Van Uitert, *Phys. Rev.* **B28**, 4774 (1983)
- [34] V Panchal, N Garg, A K Chauhan, Sangeeta and Surinder M Sharma, *Solid State Commun.* **130**, 203 (2004)

- [35] Vinod Panchal, Nandini Garg and Surinder M Sharma, *J. Phys. Condens. Matter* **18**, 3917 (2006)
- [36] D Errandonea *et al*, *Phys. Rev.* **B72**, 174106 (2005)
- [37] S Karmakar and Surinder M Sharma, *Solid State Commun.* **131**, 473 (2004)
- [38] D Oeffner and S R Elliot, *Phys. Rev.* **B58**, 14791 (1998)
- [39] V Brazhkin, A G Lyapin, R N Voloshin, S V Popova, E V Tar'yanin and N F Borovikov, *Phys. Rev. Lett.* **90**, 145503 (2003)
- [40] M Guthrie, C A Tulk, C J Benmore, J Xu, J L Yarger, D D Klug, J S Tse, H Mao and R J Hemley, *Phys. Rev. Lett.* **93**, 115502 (2004)
- [41] O Ohtaka, H Arima, H Fukui, W Utsumi, Y Katayama and A Yoshiasa, *Phys. Rev. Lett.* **92**, 155506 (2004)
- [42] K V Shanavas, Nandini Garg and Surinder M Sharma, *Phys. Rev.* **B73**, 094120 (2006)